P1.7

The 4-5 December 2001 IMPROVE-2 Event: Orographic Flow and Precipitation Structures and Evaluation of Model Microphysics

Brian A. Colle[1], Yanluan Lin[1], Christopher Woods[2], Bradley F. Smull[2]

[1] Institute for Terrestrial and Planetary Atmospheres, Stony Brook University / SUNY

[2] Department of Atmospheric Sciences, University of Washington, Seattle, WA

1. Introduction

Quantitative precipitation forecasts (QPFs) from operational models have improved relatively slowly during the past two decades. In areas of steep topography, some of the QPF problems have been attributed to deficiencies in bulk microphysical parameterizations (BMP) (Colle and Mass 2000; Garvert et al. 2005b), as well as difficulty in describing orographic forcing on 1-10 km scales (Garvert et al 2005a).

In order to verify and improve BMPs, in-situ microphysical measurements as well as thermodynamic and kinematic observations were collected during the IMPROVE project in 2001 (Stoelinga et al. 2003). Previous studies of the 13-14 December 2001 IMPROVE-2 event over central Oregaon Cascades showed snow overprediction aloft in the Penn State-NCAR Mesoscale Model (MM5), which resulted in surface precipitation overprediction in the immediate lee of the Cascades during a period of strong low-level cross barrier flow (Garvert et al. 2005a, 2005b).

This paper investigates the 4-5 December 2001 IMPROVE-2 IOP, which featured cross barrier flow (20-30 m s^{-1}) that was half as strong as the 13-14 December 2001 event. As a result, the orographic upslope forcing was less, thereby providing a useful contrast with the well-documented 13-14 December 2001 event. The goal of this study is to illustrate some of the flow and precipitation structures during this event as well as verify the Weather Research and Forecasting (WRF) model precipitation and microphysical forecasts.

2. Data and methods

WRF v2.1 was utilized to simulate the 4-5 December 2001 IMPROVE-2 event (IOP6). A MM5 v3.7 run was also completed for some comparisons. Both models used a 36-km domain with a 12-km nest that was integrated for 30 hours to simulate the large-scale features over a large area of the eastern Pacific and Pacific Northwest (not shown). The model initial and time dependent boundary conditions were derived from the NCEP GFS forecast initialized at 1200 UTC 04 December 2001. Thirty-two unevenly spaced half-sigma levels were used in the vertical, with maximum resolution in the boundary layer. Control simulations used the updated Reisner2 scheme (Thompson et al. 2004), new Kain-Fritsch cumulus parameterization, and Eta (MYJ) PBL. Model domain setup and primary physics were chosen to be as similar as possible in both MM5 and WRF simulations.

Corresponding author address: Dr. Brian A. Colle, Marine Sciences Research Center, Stony Brook University/SUNY, Stony Brook, NY 11794-5000. email: brian.colle@stonybrook.edu

A separate 4-km and 1.33 km nest centered over the study area was run for 24 hours initialized at 1200 UTC 04 December 2001 by linearly interpolating the 12-km forecast for boundary conditions. The convective parameterization was turned off for these inner domain simulations. Control MM5 and WRF simulations using the Thompson microphysical scheme (Thompson et al. 2004) were run down to 1.33 km grid spacing. Three additional BMP sensitivity tests were run with WRF using a modified Thompson scheme available on May 31, 2006 (Greg Thompson, personal communication 2006), Purdue Lin scheme (Chen and Sun 2002), and WSM-6 BMP (Hong et al. 2004) down to 4 km grid spacing.

The primary observational facilities and locations during IMPROVE-2 are described in Stoelinga et al. 2003. Microphysical measurements from NOAA P-3 and Convair aircrafts provide the opportunity for direct microphysical verification of model simulations.

3. Results

3.1 Kinematic Analusis

This IOP featured a landfalling baroclinic wave over the Pacific Northwest (not shown). Shortly before the aircraft reached the IOP region at 0100 UTC 5 December there was moist west-southwesterly flow at 15-20 m s^{-1} near crest level (800 mb) at the UW sounding site (Fig. 1; see UW on Fig. 2a). The WRF was within 5 m s^{-1} of observed below 600 mb, and the model and observed stratification was slightly more stable than moist neutral in this layer. The WRF did not simulate the shallow sub-saturated layer near the surface as well as the nearly calm winds at the lowest level.

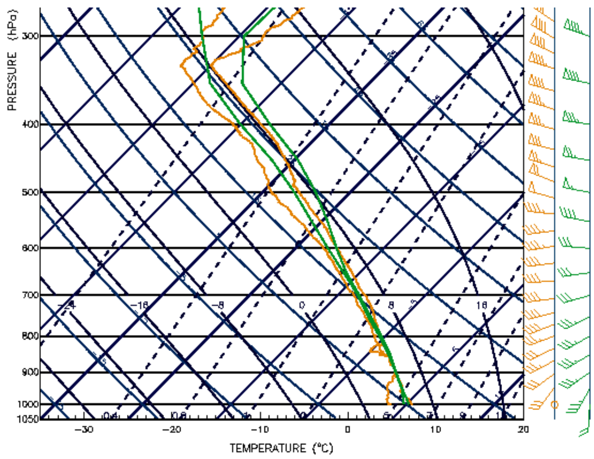

Figure 1. Observed (orange) and 1.33-km WRF (green) sounding at the UW sounding site at 0100 UTC 5 December 2001. See Fig. 2a for UW location.

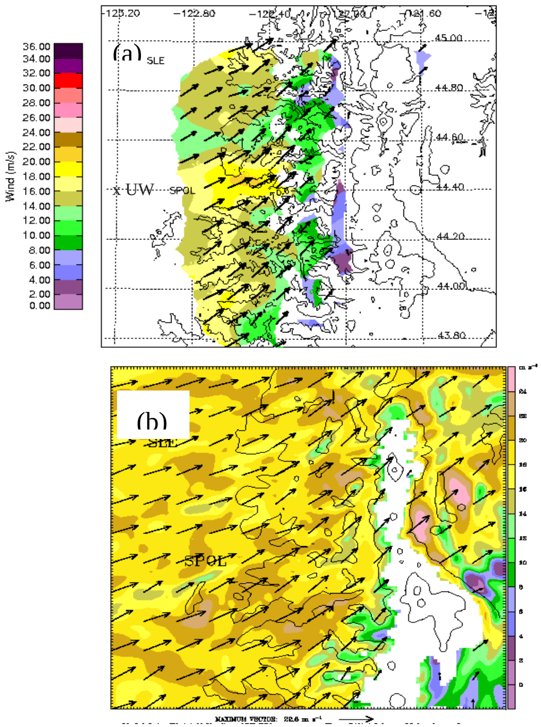

Figure 2. (a) NOAA P-3 tail-radar derived Doppler winds (m s-1) at 1.5 km ASL between 2300 UTC and 0045 UTC 5 Dec 2001. (b) Same as (a) except for the 1.33-km WRF at 00 UTC.

The simulated winds over the Cascades were compared with the Doppler winds derived from the NOAA P-3 tail radar between 2300 and 0030 UTC 5 December (Fig. 2). The observed winds at 1500 m ASL decelerated from 15-20 m s^{-1} to < 5 m s^{-1} and became more southerly towards the crest (Fig. 3a). This partially blocked flow response is consistent with the Froude number of ~1 (U~ 15 m s^{-1}, N_m ~0.005 s^{-1}, and h_m ~2000 m). The 1.33-km WRF winds at this level were 2-5 m s^{-1} too strong upstream of the Cascades. Cross section (AB) illustrates that WRF's shear in the boundary layer was too shallow as compared to the P-3 at 0200 UTC 5 December (Fig. 4). This shear layer was also not properly simulated using other WRF PBL schemes, such as the YSU and MRF (not shown). The WRF was able to simulate the wind speed increase towards the crest associated with the mountain gravity wave.

Similar to other IMPROVE-2 IOPs (Garvert et al. 2006), the southwesterly cross barrier flow produced numerous mountain (gravity) waves over the Cascade ridges, which produced vertical motion observations of +/- 1 m s^{-1} along the NOAA P-3 flight legs over the Cascades (not shown). Figure 4 shows data from segment AB on Fig. 5b at 3.1 km ASL, which compares the P-3 with the 4- and 1.33-km WRF. The 1.33-km WRF was able to generate the vertical velocity perturbations over the ridges as well as the wind speed profile over the Cascades from point B (east) to A (west). The 4-km WRF could not resolve as well the magnitude of these vertical motion fluctuations given its somewhat smoother topography. Both the 4- and 1.33-km WRF wind directions were 5-10^{o} too southwesterly at flight-level.

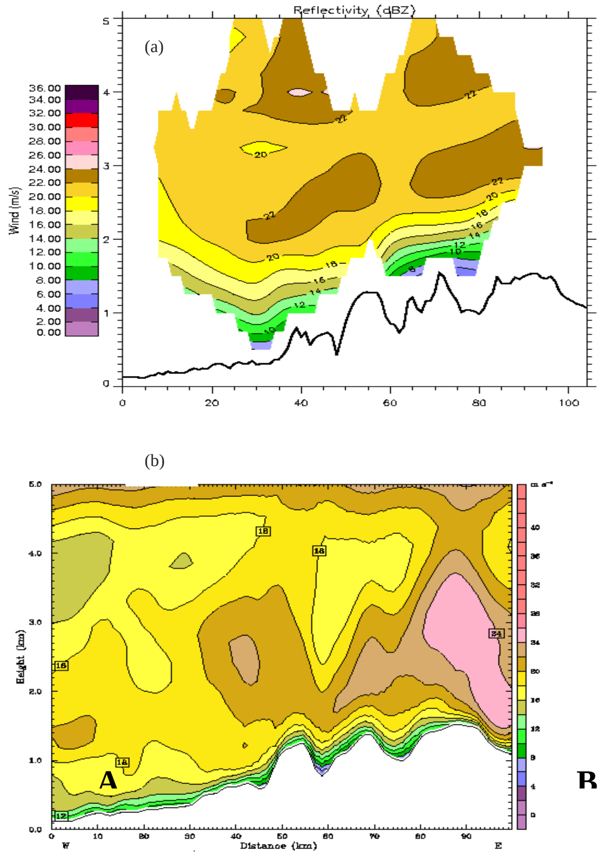

Figure 3. (a) NOAA P3 tail-radar derived Doppler wind speeds (shaded every 2 m s^{-1}) at 0200-0217 UTC 5 December along section AB in Fig. 1. (b) Same as (a) except for the 1.33-km WRF at 0200 UTC 5 December (14 h). The same color scale is used for (a) and (b).

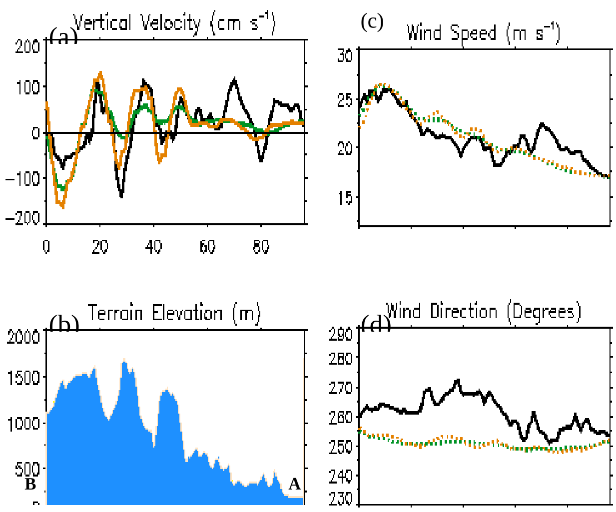

Figure 4. (a) Vertical velocity (cm s^{-1}) from the NOAA P-3 (black), 1.33-km WRF (orange), and 4-km WRF (green) between points AB in Fig. 1 at 3.1 km ASL. (b) Observed terrain profile (in m) below the flight track. (c) Same as (a) except for wind speed (m s^{-1}). (d) Same as (a) except for wind direction (in degrees).

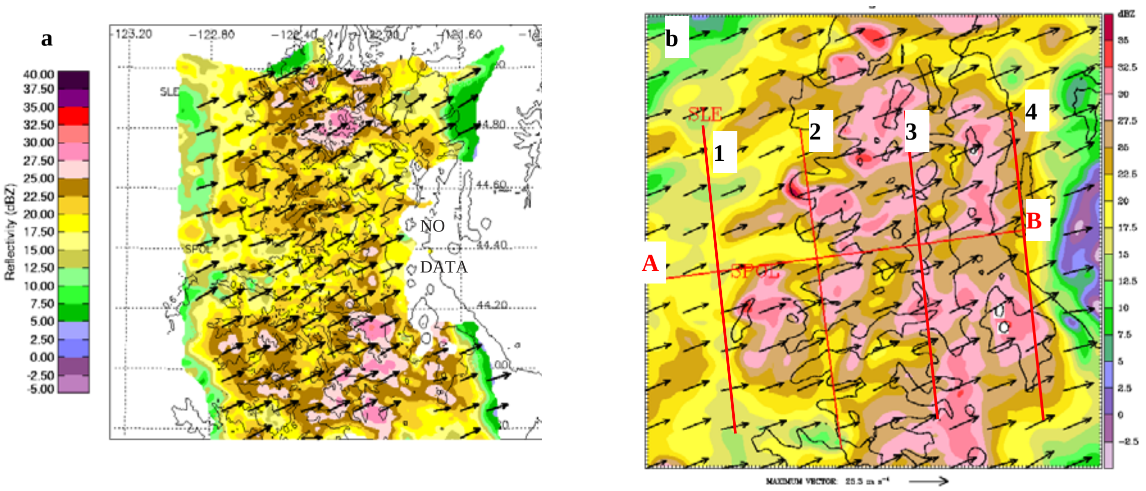

Figure 5. (a) NOAA P-3 dual Doppler reflectivities and winds at 2.5 km ASL between 2352 UTC 04 and 0057 UTC 05 December 2001. (b) Same as (a) except for the 1.33-km WRF at 0100 UTC 5 December.

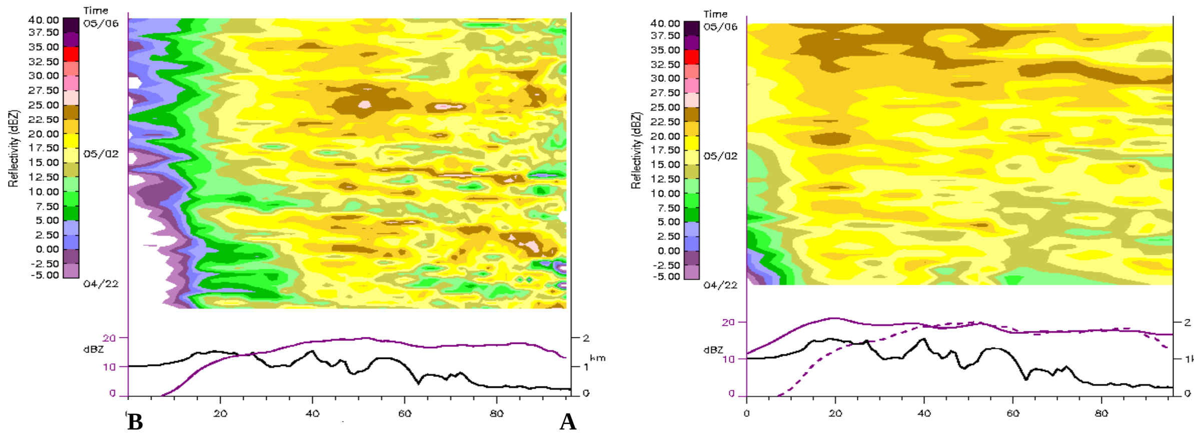

Figure 6. (a) Hovmoeller plot along AB from SPol showing reflectivities at 2-km ASL from 2200 to 0500 UTC. The terrain and average precipitation at each point along AB are shown by the black and purple lines, respectively. (b) Same as (a) except for WRF.

3.2. Precipitation and microphysical analysis

NOAA P-3 radar reflectivities and wind vectors were combined from leg2 to leg4 over the Cascades between 2352 UTC 04 and 0057 UTC 05 December 2001 following Bousquet and Smull (2003). Localized higher reflectivity cores at 2.5 km ASL are over the windward ridges as west-southwest winds interacted with the barrier (Fig. 2a). Weaker reflectivities were found over the Willamette Valley and in the lee of Cascades. The 1.33-km WRF at this level was able to simulate the upslope enhancement and localized higher dBZ values. Hovmoeller plots of SPol dBZ at 2-km ASL along AB suggest enhancement of precipitation cells over the mid-point of the Cascade windward slope (Fig. 6a,b). Meanwhile, the maximum model reflectivity was largest over the crest, with precipitation shifted 20 to 30 km too far downstream into the lee.

Figures 7a,b show the 1.33 km MM5 and WRF 12-h precipitation from 2200 UTC 04 to 1000 UTC 05 December, 2001. MM5 produced 20-30% more precipitation than WRF, especially in the north part of the Oregon Cascades.

The reasons for these differences are still under investigation, but it appears the MM5 had somewhat lower stability than WRF, and the precipitation was somewhat more convective over the barrier later in the event (not shown). The model bias score plots show overprediction in the 1.33-km MM5 (Fig. 7c,d).

In contrast, the WRF precipitation was within 20% of the observations, especially over the windward upslope region.

To verify the model microphysical fields, the 1.33-km MM5 and WRF simulated hydrometeor mixing ratio were interpolated in time and space to the P-3 flight tracks. The cloud water (CLW) measurements and mass concentrations of snow were determined using the method described by Woods et al. (2005). For the north-south leg2 in Fig. 5b from 2352 UTC 04 December to 0007 UTC 05 December 2001 (Fig. 8), there was 0.06-0.2 g m^{-3} of CLW observed, with temperatures ranging between -9 and -10 ^{o}C. MM5 overpredicted CLW, with approximately 0.10 g m^{-3} along most of the leg, while WRF predicted comparable values. The P3 ice mass concentrations were 0.15 g m^{-3}, both MM5 and WRF predicted an average value of 0.32 and 0.28 g m^{-3} of snow plus graupel.

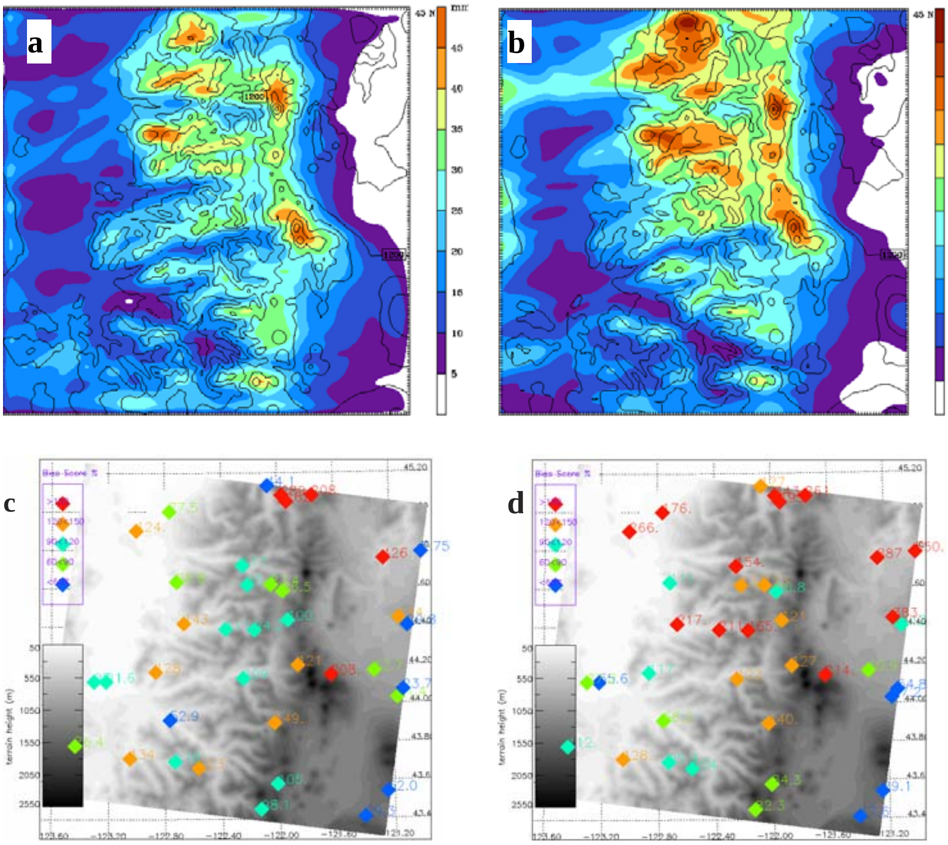

Figure 7. (a) 1.33-km WRF and (b) 1.33-km MM5 12-h precipitation total in mm between 2000 UTC 4 December and 0800 UTC 5 December (20-32h).(c) WRF and (d) MM5 1.33-km precipitation percentage of observed for the same time period in (a).

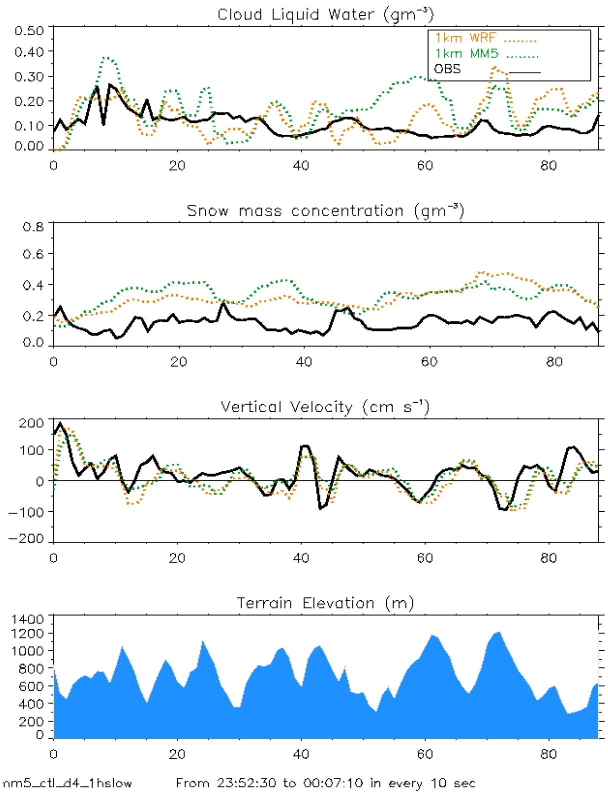

Figure 8. 1.33-km MM5 (green), WRF (orange), and observed (black) cloud water, ice (graupel and snow) mass, vertical velocity, and underlying terrain along the P-3 flight leg2.

3.2. Comparison of BMPs in WRF

To further investigate and understand BMP's sensitivity in the WRF-ARW, four different BMPs were run down to 4-km grid spacing with identical model configuration and settings as the control run except the BMPs. The schemes tested include the WSM-6 (Hong et al. 2004), Purdue-Lin (Chen and Sun 2002), Thompson (Thompson et al. 2004), and new Thompson scheme (Thompson et al., in preparation). Table 1 lists the mean CLW, snow, graupel mass concentrations along leg2 for the NOAA P3 and each BMP. The Thompson scheme overpredicted snow mass concentrations, but had comparable CLW to the observations. In contrast, the newly modified Thompson scheme (as of 25 May 2006) predicted roughly two times more snow than the Thompson in WRF V2.1. The WSM-6 predicted snow relatively well without counting cloud ice, but with much less CLW than observed, while the Purdue Lin scheme predicted too much graupel and too little snow. Clearly, there are large uncertainties in WRF microphysical schemes.

Figure 9 shows the 12-h surface precipitation totals from the four simulations. First, new Thompson predicted more precipitation than Thompson. However, less precipitation was predicted in new Thompson in the Oregon coastal range. Purdue-Lin scheme predicted a similar precipitation pattern as WSM-6, with approximately 20% larger precipitation than

WSM-6. More localized precipitation bull eyes in these two schemes are a result of more graupel. As a result, bias scores displayed more overprediction for the new Thompson and localized overprediction for WSM-6 and Lin. In addition, all the four simulations underpredicted precipitation 60-80 km downwind of Oregon Cascades crest.

Table 1. P-3 leg microphysical comparisons of four BMP simulations for legs 1-3. See Fig. 2b for leg locations.

Run name	P-3 leg1 (-6 °C, 1850 m) **snow/graupel/CLW**	P-3 leg2 (-9.5 °C, 2450 m) **snow/graupel/CLW**	P-3 leg3 (-15 °C, 3350 m) **snow/graupel/CLW**
Thompson (WRF)	**0.23/0.01/0.05**	**0.34/0.02/0.05**	**0.16/0.00/0.04**
Purdue-Lin (WRF)	**0.01/0.09/0.02**	**0.02/0.12/0.03**	**0.05/0.04/0.02**
WSM-6 (WRF)	**0.04/0.07/0.00**	**0.10/0.07/0.00**	**0.12/0.01/0.00**
New Thompson (WRF)	**0.44/0.00/0.02**	**0.54/0.00/0.02**	**0.31/0.00/0.02**
Thompson (MM5)	**0.15/0.03/0.06**	**0.26/0.03/0.06**	**0.19/0.00/0.04**
Observed	**0.05/0.02/0.06**	**0.08/0.07/0.10**	**0.06/0.01/0.03**

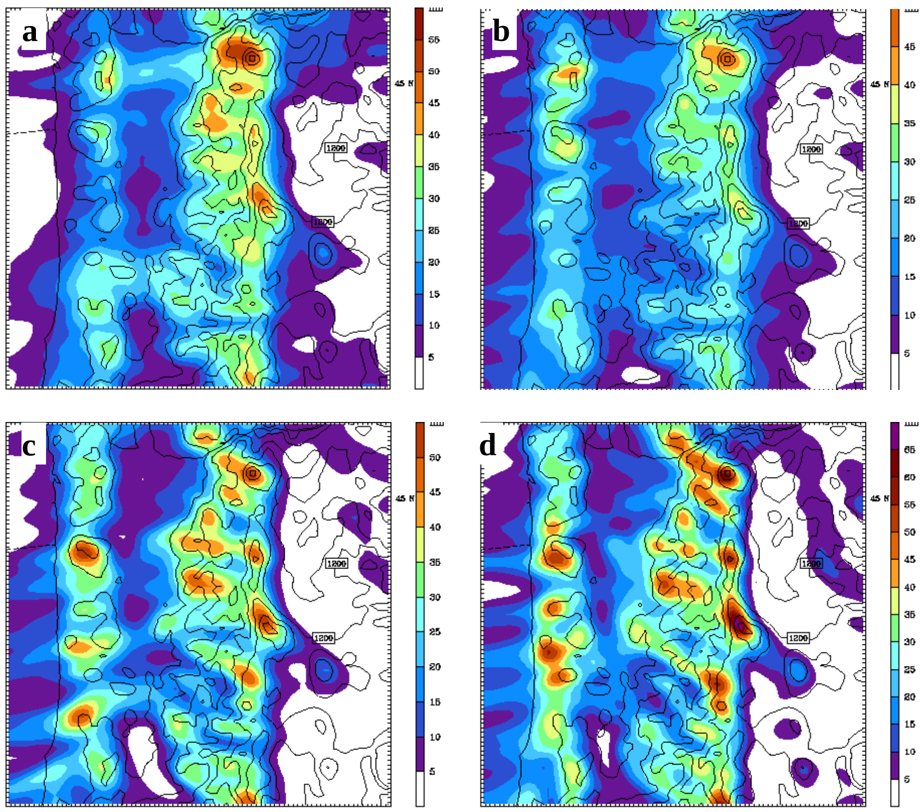

Figure 9. 2200 UTC 04 to 1000 UTC 05 December 2001 precipitation totals in mm from 4-km WRF simulation using (a) new Thompson, (b) Thompson, (c) WSM-6, and (d) Purdue Lin scheme, respectively.

Figure 10 shows the CLW, snow, graupel, rain, and cloud-ice mixing ratios (g kg^{-1}) along the UW Convair leg2 (AB in Fig. 5b) for the four BMP members. The new Thompson scheme predicted less CLW and graupel, and approximately two times more snow than the original Thompson scheme. Cloud ice is mainly above 6 km in Thompson and new Thompson, while cloud ice is more prevalent in the Lin and WSM-6 scheme. One reason might be that cloud ice is converted to snow at smaller sizes in the Thompson scheme. Compared with UW Convair measured ice mass (indicated as numbers in Fig. 10b), Thompson scheme showed slightly underprediction of snow above 4 km ASL.

5. Summary

This paper has presented some of the kinematic and precipitation structures observed during 4-5 December 2001 of IMPROVE-2. The results suggest the importance of small-scale terrain features on the precipitation. The WRF-Thompson did produce a good short-term precipitation forecast, but apparently for the wrong microphysical reasons aloft, considering that the snow was overpredicted around 2-3 km and in the lee. Both the WRF and MM5 simulations used the same version of Thompson, but MM5 generated much more precipitation and had surface overprediction. The divergence in the forecast between WRF and MM5 shows that the oropgraphic precipitation predictability for this case goes beyond microphysics. There are large precipitation differences among The WRF BMP schemes, which produce precipitation differences as large as MM5 versus WRF using the Thompson scheme. Future work will more closely evaluate the microphysical pathways for these schemes.

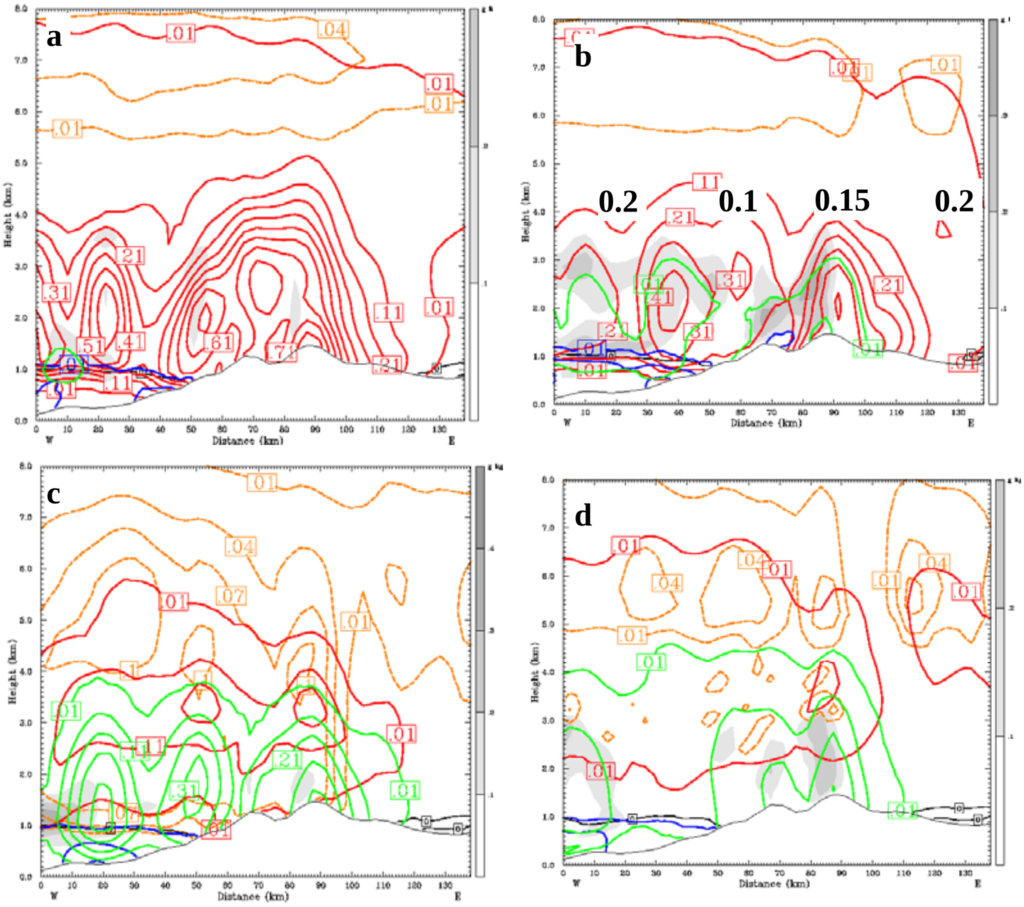

Figure 10. Cloud water (gray shaded), cloud ice (dashed orange), snow (red solid), graupel (green solid), rain (blue solid), and freezing level (black solid) along the cross section of line AB in Fig. 2b at 0200 UTC 05 December 2001 from simulations using (a) new Thompson, (b) Thompson, (c) WSM-6, and (d) Purdue Lin scheme, respectively. The numbers in (b) displayed UW Convair measured ice mass (g m^{-3}) at 4.25 km ASL.

6. Acknowledgements

This work was sponsored by the National Science Foundation.

7. References

Bousquet, O. and B.F., Smull, 2003:Airflow and precipitation fields within deep Alpine valleys observed by airborne Doppler radar. *J. Appl.Meteor.*, **42**, 1497–1513.

Colle, B. A., and C. F. Mass, 2000: The 5–9 February 1996 flooding event over the Pacific Northwest: Sensitivity studies and evaluation of the MM5 precipitation forecasts. *Mon. Wea. Rev.*, **128**, 593–617.

Colle, B. A., M. F. Garvert, J. B. Wolfe, C. F. Mass and C. P. Woods, 2005: The 13–14 December2001 IMPROVE-2Event. Part III: Simulated microphysical budgets and sensitivity studies. *J. Atmos.Sci.*,**62**, 3535–3558.

Garvert, M. F., B. A. Colle, and C. F. Mass, 2005a: The 13–14 December 2001 IMPROVE-2 event. PartI: Synoptic and mesoscale evolution and comparison with a mesoscale model simulation. *J. Atmos.Sci.*,**62**, 3474–3492.

Garvert, M. F., C. P. Woods, B. A. Colle, C. F. Mass, P. V. Hobbs, M. P. Stoelinga, and J. B. Wolfe, 2005b: The 13–14 December 2001 IMPROVE-2 event. Part II: Comparison of MM5 model simulations of clouds and precipitation with observations. *J. Atmos. Sci.*, **62**, 3520–3534.

Hong, S.-Y., Dudhia J., and S. H. Chen, 2004: A revised approach to ice microphysical processes for the bulk parameterization of clouds and precipitation. *Mon. Wea. Rev.*, **132**, 103–120.

Stoelinga, M., and Coauthors, 2003: Improvement of Microphysical Parameterization through Observational Verification Experiments. *Bull. Amer. Meteor. Soc.*, **84**, 1807–1826.

Thompson, G., R. M. Rasmussen, and K. Manning, 2004: Explicit forecasts of winter precipitation usingan improved bulk microphysics scheme. PartI: Description and sensitivity analysis. *Mon. Wea. Rev.*, **132**, 519–542.

Woods, C. P., M. Stoelinga, J. Locatelli, and P. Hobbs, 2005: Microphysical processes and synergistic interaction between frontal and orographic forcing of precipitation during the 13 December 2001 IMPROVE-2 event. *J. Atmos. Sci.*, **62**, 3493–3519.